Technical Physics Letters, 2022, Vol. 48, No. 6

07

Spin mixing conductance of the iridate/manganite interface

© *G.A. Ovsyannikov*[1], *K.I. Constantinyan*[1], *E.A. Kalachev*[2], *A.A. Klimov*[1,2]

[1] Kotelnikov Institute of Radio Engineering and Electronics, Russian Academy of Sciences, Moscow, Russia
[2] Russian Technological University (MIREA), Moscow, Russia
E-mail: gena@hitech.cplire.ru

Received March 14, 2022
Revised May 5, 2022
Accepted May 6, 2022

The results of studies of ferromagnetic resonance (FMR) of iridate/manganite epitaxial heterostructures in a wide range of microwave frequencies (1−20 GHz) are presented. The magnitudes of imaginary and real parts of the spin mixing conductance of the heterostructure boundary determining the spin current were determined from the frequency dependence of the spin damping and changes in the resonance field of the FMR. It is shown that the value of the imaginary part of spin conductance is comparable to the real part, which may be caused by strong spin−orbit interaction occurring in 5d−oxides of transition metals (iridate).

Keywords: ferromagnetic resonance, $SrIrO_3/La_{0.7}Sr_{0.3}MnO_3$ heterostructures, spin current, spin mixing conductance.

DOI: 10.21883/TPL.2022.06.53796.19187

Using in microelectronics spins instead of electron charges makes it possible to solve the problem of heat release from submicron elements since the spin transfer does not induce energy dissipation. However, the spin current detection and generation require such an approach to the problem of the spin torque transport and detection which is different from that in the case of charge transport. Most promising is the approach in which the pure (free of charge transport) spin current is generated due to ferromagnetic resonance in the ferromagnetic of the ferromagnetic/normal (nonmagnetic) metal structure, while the detection becomes possible due to the spin current conversion into the charge current under the inverse Hall spin effect in a metal with strong spin−orbit interaction [1–8].

Excitation of ferromagnetic resonance (FMR) induces in a ferromagnetic film the cross−boundary spin current. In experiments, this spin current is typically detected via the electric voltage arising due to the inverse Hall spin effect. Density of the spin current through the heterostructure interface is determined by the real ($\mathrm{Re}g^{\uparrow\downarrow}$) and imaginary ($\mathrm{Im}g^{\uparrow\downarrow}$) components of the interface spin mixing conductance, which induce an increase in the spin damping and shift of the FMR resonance frequency, respectively [3,6–8]. The $\mathrm{Im}g^{\uparrow\downarrow}$ component in diffusion and ballistic contacts is typically neglected [3,7]. Accounting for the spin mixing conductance imaginary part was performed for a double−layer Py/Pt structure in [9]. The shift of the FMR resonance frequency was observed in the Pt/YIG heterostructures and was explained by the ferromagnetic ordering of Pt atoms near the Pt/YIG interface [10]. Both components of the spin mixing conductance were experimentally determined in [11] for structure Pt/Finemet ($Fe_{66.5}CuNb_3Si_{13.5}B_6Al_7$) by using the ferromagnetic resonance dependence on frequency. It was shown experimentally that the imaginary part of the interface spin mixing conductance is defined by the interface electronic structure associated with its resistance, and also by the spin diffusion magnitude [11].

This paper presents the results on experimental determination of the real and imaginary parts of the interface spin mixing conductance of the iridate/manganite ($SrIrO_3/La_{0.7}Sr_{0.3}MnO_3$) heterostructure grown epitaxially *in situ* on the neodymium gallate (110) $NdGaO_3$ substrate. Contrary to the known case of Pt/YIG, in our case we succeeded in realizing an epitaxial interface with reproducible parameters and high spin mixing conductance. Strong spin−orbit interaction in iridate promotes efficient conversion of the spin current to the charge current, which makes easier experimental observation of the spin current generation and detection.

Nanometer epitaxial films of iridate $SrIrO_3$ (SIO3) and manganite $La_{0.7}Sr_{0.3}MnO_3$ (LSMO) were deposited on monocrystalline substrates of neodymium gallate (110) $NdGaO_3$. The epitaxial films were grown by magnetron sputtering at the substrate temperatures of 770−800°C in the Ar / O_2 gas mixture with the total pressure of 0.3−0.5 mbar [4,5].

Investigation of the crystalline structure of obtained heterostructures by the X-ray analysis and transmission electron microscopy showed that the heterostructures were grown via the „cube-on-cube“ mechanism with the following epitaxial ratios [5,12]:

$$(001)SrIrO_3||(001)La_{0.7}Sr_{0.3}MnO_3||(110)NdGaO_3,$$

$$[100]SrIrO_3||[100]La_{0.7}Sr_{0.3}MnO_3||[001]NdGaO_3.$$

The transient layer on the SIO3/LSMO interface consisted of 1−2 atomic layers, above which the growth of a uniform film was observed.

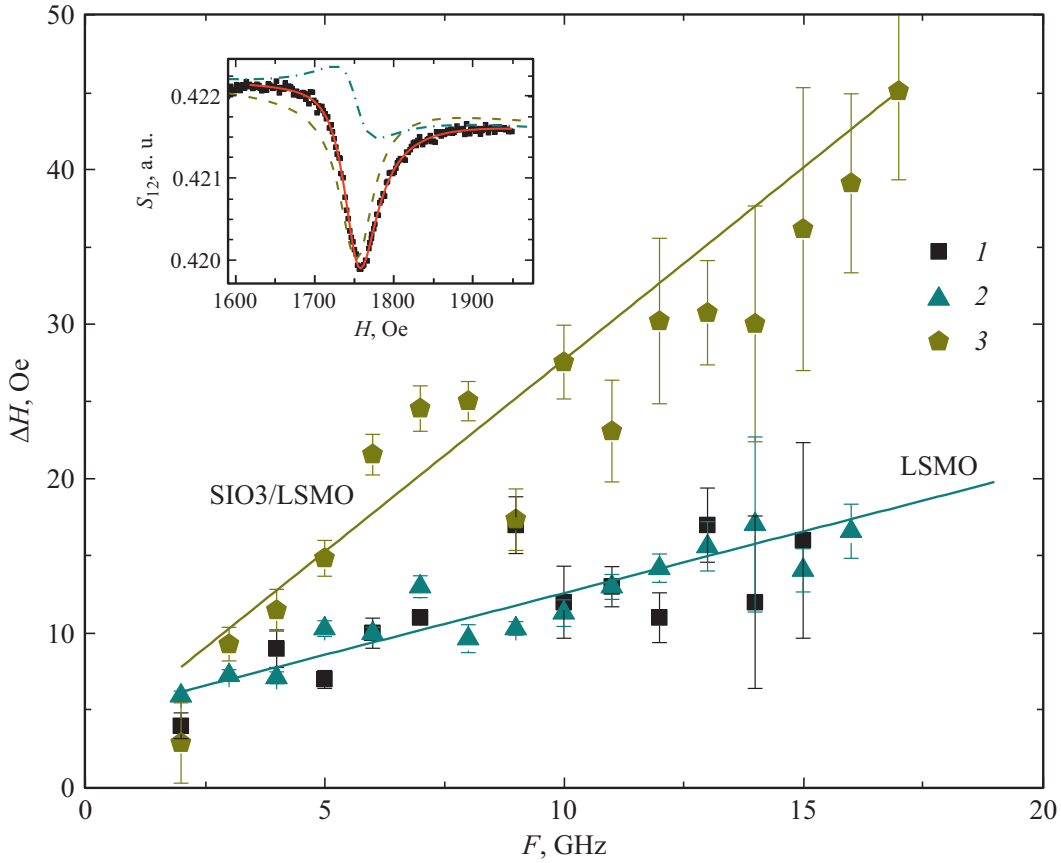

Figure 1. Frequency F dependence of the FMR line width ΔH for two LSMO films ($1, 2$) and heterostructure SIO3/LSMO (3). Solid lines represent linear approximations of experimental data. The inset presents spectrum $S_{12}(H)$ of the heterostructure exposed to the $F = 9$ GHz microwave radiation. The solid line represents the spectrum approximation with a sum of the Lorenz line (dashed line) and dispersion characteristic (dot–and–dash line).

The FMR spectrum was determined based on the magnetic–field dependence of the transmitting microwave radiation amplitude $S_{12}(H)$ in the frequency band $F = 1–20$ GHz. The $S_{12}(H)$ spectrum shape (Fig 1, inset) was approximated with the Lorenz line accounting for the imaginary component of the ferromagnetic magnetic susceptibility and with the dispersion characteristic for its real part [13]. By fitting the experimental data with a sum of these two components and also with the linear magnetic field dependence $S_{12}(H)$, one can succeed in determining the resonance field H_0 and Lorenz line width ΔH. In the experiment, the spin damping is characterized by parameter ΔH, while the gyromagnetic ratio γ determines the resonance magnetic field H_0 based on the Kittel relations taking into account the LSMO film magnetization and magnetic anisotropy.

Fig. 1 demonstrates the ΔH dependences on the microwave frequency, which were obtained from the spectra for the LSMO film and heterostructure. Contrary to the $H_0(F)$ dependences (Fig. 2), here a rather great dispersion of measurements is observed even for one and the same measured sample. The Gilbert spin damping parameter α and line broadening caused by the ΔH_0 non–uniformity may be determined using relation $\Delta H(F) = 4\pi\alpha F/\gamma + \Delta H_0$. In this case, other sources of spin damping are ignored (see, e. g., [14]).

As Fig. 1 shows, parameter α for the LSMO film

$$\alpha_{\mathrm{LSMO}} = 2.0 \pm 0.2 \cdot 10^{-4}$$

increases due to deposition of SIO3 to

$$\alpha_{\mathrm{SIO3/LSMO}} = 6.7 \pm 0.8 \cdot 10^{-4}.$$

The damping magnitude $\Delta H_0 = 6$ Oe caused by the ferromagnetic inhomogeneities is low and does not significantly affect the spin current, especially at high (more than 10 GHz) frequencies. The value of the spin mixing conductance real part is defined as follows [3,11]:

$$\mathrm{Re}g^{\uparrow\downarrow} = \frac{4\pi M_0 d_F}{g_0 \mu_{\mathrm{B}}}\left(\alpha_{\mathrm{SIO3/LSMO}} - \alpha_{\mathrm{LSMO}}\right), \qquad (1)$$

where $\mu_{\mathrm{B}} = 9.274 \cdot 10^{-21}$ erg/G is the Bohr magneton, $g_0 = 2$ is the free–electron Lande factor, $d_F = 30$ nm is the LSMO film thickness, M_0 is the

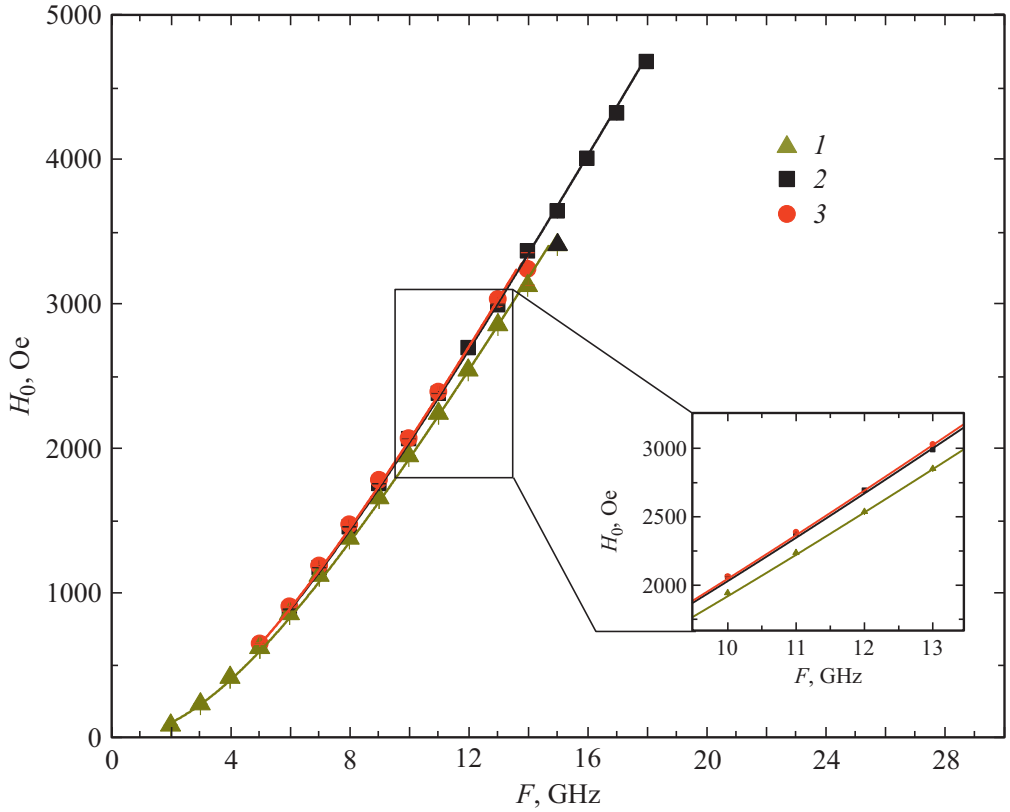

Figure 2. The FMR resonance field H_0 versus microwave frequency F for three structures: the LSMO film (1) and two SIO3/LSMO heterostructures ($2,3$). In both cases, the SIO3 and LSMO thicknesses are 10 and 30 nm, respectively. Measurement errors do not exceed the sizes of experimental points. Solid lines represent the $H_0(F)$ dependences according to the Kittel formula (2) for a ferromagnetic with uniaxial anisotropy at the magnetic field aligned with the easy−magnetization axis. The range of the $H_0(F)$ variation is shown in the inset in the magnified view.

saturation magnetization. The increase in difference $\alpha_{\mathrm{SIO3/LSMO}} - \alpha_{\mathrm{LSMO}}$ for the SIO3/LSMO heterostructure gives $\mathrm{Re}g_{eff}^{\uparrow\downarrow} = (3.6 \pm 0.5) \cdot 10^{19}\,\mathrm{m}^{-2}$. Notice that value $\mathrm{Re}g_{eff}^{\uparrow\downarrow} = 1.3 \cdot 10^{18}\,\mathrm{m}^{-2}$ was obtained in [15] for heterostructure SIO3/LSMO fabricated by laser ablation. According to the data given in [16], variation in the SIO3 film thickness from 10 to 40 nm causes the heterostructureś $\mathrm{Re}g_{eff}^{\uparrow\downarrow}$ variation from $1.3 \cdot 10^{19}$ to $3.6 \cdot 10^{19}\,\mathrm{m}^{-2}$, respectively, which is close to our value.

Fig. 2 presents the resonance field H_0 dependences on the microwave frequency F for the LSMO film and two SIO3/LSMO heterostructures in the magnetic field aligned with the easy−magnetization axis. Measurements of the room−temperature LSMO film angular dependences show [5,17] that the cubic anisotropy is negligible, while magnetization M_0 and uniaxial magnetic anisotropy H_u differ slightly from those obtained from dependence $H_0(F)$

$$F = \gamma(4\pi M_0 + H_u + H_0)^{1/2}(H_0 + H_u)^{1/2} \qquad (2)$$

in the magnetic field aligned with the easy−magnetization axis. At high frequencies (above 10 GHz), the heterostructures exhibit a deviation of the $H_0(F)$ dependence from $H_0(F)$ for the LSMO films (Fig. 2). The deviation may be caused by either the M_0 and H_u variations in the heterostructure or by the γ variation due to existence of component $\mathrm{Im}g^{\uparrow\downarrow}$ in the heterostructure γ (see relation (3) below). The Fig. 2 inset shows that a decrease in H_0 is observed at a fixed frequency. In order to determine the γ variation caused by depositing SIO3 over the LSMO film, we have fitted the $H_0(F)$ dependences by relation (2) for the heterostructures and LSMO films. Here we assumed that the LSMO film magnetization $M_0 = 370$ Oe and magnetic anisotropy $H_u = 11$ Oe providing the best agreement of experimental data with (2) had not changed after the SIO3 deposition over the LSMO film. Relative variation $\delta\gamma/\gamma_0 = 0.036 \pm 0.001$ caused by the SIO3 deposition over the LSMO film is determined by $\mathrm{Im}g^{\uparrow\downarrow}$ [3,10]:

$$\delta\gamma/\gamma_0 = \mathrm{Im}g^{\uparrow\downarrow}\frac{g_0\mu}{4\pi M_S d_F}. \qquad (3)$$

For the heterostructure presented in Fig. 2, obtain

$$\mathrm{Im}g^{\uparrow\downarrow} = (46 \pm 1) \cdot 10^{19}\,\mathrm{m}^{-2}.$$

As shown in [6,11,18], $\mathrm{Re}g^{\uparrow\downarrow}$ is defined mainly by normal−metal parameters: specific resistance and spin function length. At the same time, $\mathrm{Im}g^{\uparrow\downarrow}$ depends on

the properties of ferromagnetic/normal–metal interface; thereat, an important role is played by the magnitude of the spin–orbit interaction and the interface quality [11]. It is possible that the $\mathrm{Im}g^{\uparrow\downarrow}$ estimation via formula (3) is affected by the emergence of magnetization directed normally to the interface, which was observed in the manganite/iridate superlattices [19].

Thus, values of the real and imaginary parts of the spin mixing conductance of the heterostructure boundary which define the cross–boundary spin current were obtained based on the results of studying the ferromagnetic resonance in epitaxial heterostructures $SrIrO_3/La_{0.7}Sr_{0.3}MnO_3$ in a wide microwave frequency band (1–20 GHz). The imaginary part of spin mixing conductance appeared to be abnormally high (higher than that in the case of heterostructures with platinum).

Acknowledgements

The authors are grateful to T.A. Shaikhulov for preparing thin epitaxial films of manganite and heterostructures, and also to V.V. Demidov, K.A. Stankevich and A.M. Petrzhik for the assistance in measurements and for useful discussion of experimental results.

Fionancial support

The study was accomplished in the framework of State Assignment for Kotelnikov IRE of RAS. The study was performed by using the equipment of Unique Research Facility № 352529 „Cryointegral“whose development was supported by the grant of RF Ministry of Science and Higher Education (contract № 075-15-2021-667). Development of the microwave measurement technique by A.A. Klimov was supported by the Russian Scientific Foundation (project № 20-12-00276).

Conflict of interests

The authors declare that they have no conflict of interests.

References

[1] E. Saitoh, M. Ueda, H. Miyajima, G. Tatara, Appl. Phys. Lett., **88**, 182509 (2006). DOI: 10.1063/1.2199473
[2] O. Mosendz, V. Vlaminck, J.E. Pearson, F.Y. Fradin, G.E.W. Bauer, S.D. Bader, A. Hoffmann, Phys. Rev. B, **82**, 214403 (2010). DOI: 10.1103/PhysRevB.82.214403
[3] Ya. Tserkovnyak, A. Brataas, G.E.W. Bauer, Phys. Rev. Lett., **88**, 117601 (2002). DOI: 10.1103/PhysRevLett.88.117601
[4] .A. Shaikhulov, G.A. Ovsyannikov, V.V. Demidov, N.V. Andreev, JETP, **129**, 112 (2019). DOI: 10.1134/S1063776119060153.
[5] G.A. Ovsyannikov, T.A. Shaikhulov, K.L. Stankevich, Yu. Khaydukov, N.V. Andreev, Phys. Rev. B, **102**, 14440 (2020). DOI: 10.1103/PhysRevB.102.144401
[6] M. Zwierzycki, Y. Tserkovnyak, P.J. Kelly, A. Brataas, G.E.W. Bauer, Phys. Rev. B, **71**, 064420 (2005). DOI: 10.1103/PhysRevB.71.064420
[7] V.P. Amin, M.D. Stiles, Phys. Rev. B, **94**, 104420 (2016). DOI: 10.1103/PhysRevB.94.104420
[8] K.-W. Kim, K.-J. Lee, J. Sinova, H.-W. Lee, M.D. Stiles, Phys. Rev. B, **96**, 104438 (2017). DOI: 10.1103/PhysRevB.96.104438
[9] T. Nan, S. Emori, C.T. Boone, X. Wang, T.M. Oxholm, J.G. Jones, B.M. Howe, G.J. Brown, N.X. Sun, Phys. Rev. B, **91**, 214416 (2015). DOI: 10.1103/PhysRevB.91.214416
[10] Y. Sun, H. Chang, M. Kabatek, Y.-Y. Song, Z. Wang, M. Jantz, W. Schneider, M. Wu, E. Montoya, B. Kardasz, B. Heinrich, G.E.S. te Velthuis, H. Schultheiss, A. Hoffmann, Phys. Rev. Lett., **111**, 106601 (2013). DOI: 10.1103/PhysRevLett.111.106601
[11] J. Dubowik, P. Graczyk, A. Krysztofik, H. Głowinski, E. Coy, K. Załeski, I. Goscianska, Phys. Rev. Appl., **13**, 054011 (2020). DOI: 10.1103/PhysRevApplied.13.054011
[12] G.A. Ovsyannikov, K.I. Constantinyan, V.A. Shmakov, A.V. Shadrin, Y.V. Kislinsky, N.V. Andreev, F.O. Milovich, A.P. Orlov, P.V. Lega, Radioelektronika. Nanosistemy. Informatsionnye tekhnologii, **13** (4), 479 (2021). DOI: 10.17725/rensit.2021.13.479 (in Russian)
[13] M. Harder, Z.X. Cao, Y.S. Gui, X.L. Fan, C.-M. Hu, Phys. Rev. B, **84**, 054423 (2011). DOI: 10.1103/PhysRevB.84.054423
[14] T.A. Shaikhulov, G.A. Ovsyannikov, Phys. Solid State, **60**, 2231 (2018). DOI: 10.1134/S1063783418110288.
[15] S. Crossley, A.G. Swartz, K. Nishio, Y. Hikita, H.Y. Hwang, Phys. Rev. B., **100**, 115163 (2019). DOI: 10.1103/PhysRevB.100.115163
[16] X. Huang, S. Sayed, J. Mittelstaedt, S. Susarla, S. Karimeddiny, L. Caretta, H. Zhang, V.A. Stoica, T. Gosavi, F. Mahfouzi, Q. Sun, P. Ercius, N. Kioussis, S. Salahuddin, D.C. Ralph, R. Ramesh, Adv. Mater., **33**, 2008269 (2021). DOI: 10.1002/adma.202008269
[17] V.V. Demidov, T.A. Shaikhulov, G.A. Ovsyannikov, J. Magn. Magn. Mater., **497**, 165979 (2020). DOI: 10.1016/j.jmmm.2019.165979
[18] F.D. Czeschka, L. Dreher, M.S. Brandt, M. Weiler, M. Althammer, I.-M. Imort, G. Reiss, A. Thomas, W. Schoch, W. Limmer, H. Huebl, R. Gross, S.T.B. Goennenwein, Phys. Rev. Lett., **107**, 046601 (2011). DOI: 10.1103/PhysRevLett.107.046601
[19] D. Yi, H. Amari, P.P. Balakrishnan, C. Klewe, A.T. N'Diaye, P. Shafer, N. Browning, Y. Suzuki, Phys. Rev. Appl., **15**, 024001 (2021). DOI: 10.1103/PhysRevApplied.15.024001